Probe Selection in Multiprobe OTA Setups

Fan, Wei; Sun, Fan; Nielsen, Jesper Ødum; Carreño, Xavier; Ashta, Jagjit Singh ; Knudsen, Mikael Bergholz; Pedersen, Gert Frølund

Published in:
I E E E Transactions on Antennas and Propagation

DOI (link to publication from Publisher):
10.1109/TAP.2014.2301179

Publication date:
2014

Document Version
Early version, also known as pre-print

This article has been accepted for publication in a future issue of this journal, but has not been fully edited. Content may change prior to final publication. Citation information: DOI 10.1109/TAP.2014.2301179, IEEE Transactions on Antennas and Propagation

Probe Selection in Multi-probe OTA Setups

Wei Fan, Fan Sun, Jesper Ø. Nielsen, Xavier Carreño, Jagjit S. Ashta, Mikael B. Knudsen and Gert F. Pedersen

***Abstract*—Standardization work for over-the-air (OTA) testing of multiple input multiple output (MIMO) capable terminals is currently ongoing in COST IC1004, 3GPP and CTIA, where a multi-probe anechoic chamber based method is a promising candidate. Setting up a multi-probe configuration with channel emulators is costly, so finding ways to limit the number of probes while still reproducing the target channels accurately could make the test system both cheaper and simpler to implement. Several probe selection algorithms are presented in this paper to address this issue. The proposed techniques provide a probe selection framework for the channel emulation techniques published in the literature. Simulation results show that good channel emulation accuracy can be achieved with the selected subset of probes for the considered target channel models. The probe selection algorithm is further supported by measurement results in a practical multi-probe setup.**

I. Introduction

Over-the-air (OTA) testing of the radio performance of mobile terminals has the advantage of not needing to break or otherwise modify the mobile device. OTA testing for mobile terminals with a single antenna was standardized by CTIA and 3GPP about ten years ago, but these standards cannot be used directly for evaluating multiple input multiple output (MIMO) capable devices [1]. OTA testing for MIMO capable terminals is mandatory as traditional conductive tests bypass the antennas and thus results in unrealistic performance evaluation results. There are three main types of OTA test methods for MIMO devices: multi-probe anechoic chamber-based methods, reverberation chamber-based methods and two-stage methods [1]. All currently have their limitations: there is limited temporal and spatial control of the reproduced channel in the reverberation chamber-based method; practical issues such as including self-interference still exist in the two-stage method; and the cost of the setup is the main issue with the multi-probe anechoic chamber-based method [1].

Several papers have addressed OTA testing for MIMO devices in multi-probe anechoic chamber setups with emphasis on channel modeling, where the goal is to accurately reproduce realistic channel models in the test volume. Two channel emulation techniques have been proposed in the literature. One technique is the plane wave synthesis (PWS) technique reported in [2]–[4]. The other technique is named the prefaded signal synthesis (PFS) technique [2] and has been adopted in several commercial channel emulators, e.g. Anite Propsim channel emulation solutions and Spirent VR5 [5], [6]. Verification measurements of the two techniques in a two dimensional (2D) multi-probe setup have been reported in many contributions, see e.g. [7]–[10]. It has been shown that the channels reproduced in the test area match well with the target. To emulate a realistic environment which can accurately reflect the real wireless propagation environment in the anechoic chamber, 3D channel model emulation with the multi-probe setup in an anechoic chamber has attracted interest as well [4], [11]–[13].

The cost of the multi-probe anechoic chamber setup mainly depends on the channel emulators and the number of probes required for reproducing the desired channel models. It has been demonstrated that a large number of probes is required to create a large test area in the chamber [11], [12], [14]. As the number of available output ports of the channel emulator is limited, several channel emulators are often required, which will dramatically increase the setup cost. Setting up a 3D multi-probe configuration is even more costly, so finding ways to limit the number of probes while still approximating the target channels sufficiently accurately could make the test system both cheaper and simpler to implement. Radio channel models are generally directional in real world scenarios, which has been widely studied in the literature and adopted in the standard channel models, see e.g. [15]–[18]. However, a uniform configuration of the OTA probes over the azimuth plane is often adopted in the multi-probe setup [1]. As a consequence, contributions from some probes might be dominant, while negligible from other probes when synthesizing the target radio channels. Hence a probe selection mechanism has potential to save cost, via reducing the required number of fading channels.

Figure 1 shows an illustration of a practical 3D multi-probe setup, where a probe selector is used to select the optimal subset of probes for reproducing the desired channels. The basic idea is to select an optimal subset of probes of size N from K total available probes ($N \leq K$). The N selected probes are connected to the PAs and the channel emulators and hence are used for reproducing the target channels in the test zone, while the other probes are disconnected from the channel emulator and properly terminated.

The probe selection technique for 2D single cluster spatial channel models has been implemented in a commercial channel emulator, the Anite Propsim channel emulator. In [19], the probe selection algorithm in 2D multi-probe setups was briefly described for the PFS technique, although no results were given.

In this paper, the probe selection in a 3D multi-probe OTA setup is addressed, where the probes are selected based on channel emulation accuracy in terms of either field synthesis error or spatial correlation error, which are selected as the figure of merit (FoM) in the PWS and the PFS technique,

Wei Fan, Fan Sun, Jesper Ø. Nielsen, and Gert F. Pedersen are with the Antennas, Propagation and Radio Networking section at the Department of Electronic Systems, Faculty of Engineering and Science, Aalborg University, Denmark (email: {wfa, fs, jni, gfp}@es.aau.dk).

Xavier Carreño, Jagjit S. Ashta, and Mikael B. Knudsen are with Intel Mobile Communications, Denmark (email: {xavier.carreno, jagjitx.singh.ashta, mikael.knudsen}@intel.com).

This article has been accepted for publication in a future issue of this journal, but has not been fully edited. Content may change prior to final publication. Citation information: DOI 10.1109/TAP.2014.2301179, IEEE Transactions on Antennas and Propagation

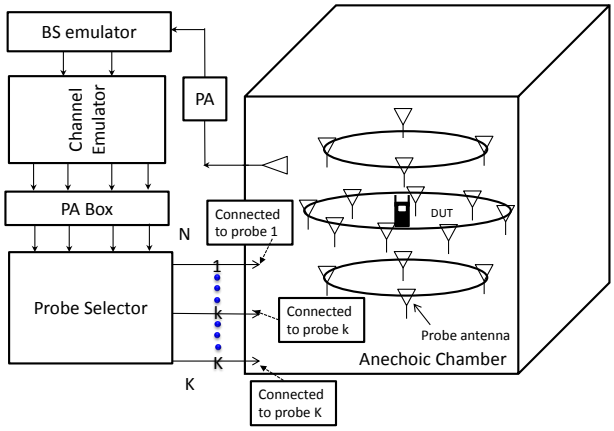

Figure 1. An illustration of the probe selection in a multi-probe setup. The system consists of a base station (BS) emulator, one or several radio channel emulators, an anechoic chamber, OTA probe antennas, a power amplifier (PA) box, a probe selector and a device under test (DUT). K and N denote the number of available OTA probes and the number of active OTA probes that are connected to the channel emulator, respectively.

respectively [2], [20]. The main contributions of this work are:

- We form the probe selection algorithms both for the PWS and the PFS techniques.
- The probe selection algorithm for multi-cluster channel models is proposed.
- We propose the probe selection algorithm for 3D multi-probe setups with arbitrary probe configurations.
- Three different probe selection algorithms are proposed and evaluated.
- The probe selection algorithm for a multi-cluster channel model is supported by measurements in a practical 2D multi-probe setup.

II. Channel Emulation Techniques

A. Prefaded signal synthesis (PFS)

The PFS technique was proposed in [2] for the 2D multi-probe setup and was extended to the 3D multi-probe setup in [11]. As detailed in [11], the focus is on reproducing the channel spatial characteristics in the test volume at the receiver (Rx). The basic idea is that by allocating appropriate power weights to the OTA probes, we can reproduce the incoming spherical power spectrum (SPS) of the channel in the test volume. The goal is to minimize the deviation between the theoretical spatial correlation resulting from the target continuous SPS, and the emulated spatial correlation resulting from the discrete SPS, with its shape characterized by the discrete angular positions of the probes and the power weights.

A location pair is used to represent the locations of two spatial samples where the two isotropic antennas u and v are placed [11], [21]. The two spatial samples are selected to be directly opposite to each other w.r.t the test volume center and the distance between them is the test volume size. It is desirable that the spatial correlation error $|\rho - \hat{\rho}|$ should be smaller than the predefined emulation accuracy requirement for all the location pairs. The DUT should be smaller than the test volume size to ensure that the target propagation environment is accurately reproduced around the DUT. As explained in [2], [11], the polarization is omitted from the described PFS method, as the SPS of target channel models for different polarizations can be reproduced applying the same PFS technique. Probe selection for the dual polarized channel models should be based on the cross polarization ratio (XPR) of the channel models.

The spatial correlation for the mth location pair can be determined according to [11], for a single polarization, as:

$$\rho(m) = \oint \exp(ja(\overline{r}_{u,m} - \overline{r}_{v,m}) \cdot \overline{\Omega}) p(\Omega) d\Omega, \qquad (1)$$

where $\overline{r}_{u,m}$ and $\overline{r}_{v,m}$ are vectors containing the position information of antenna u and v at the mth location pair, respectively. $\overline{\Omega}$ is an unit vector corresponding to the solid angle Ω. a is the wave number. $p(\Omega)$ is the SPS satisfying $\oint p(\Omega) d\Omega = 1$. $(\cdot)$ is the dot product operator. Similar to (1), the emulated spatial correlation for the mth location pair can be calculated based on the discrete SPS characterized by K probes as:

$$\hat{\rho}(m) = \sum_{k=1}^{K} w_k \exp(ja(\overline{r}_{u,m} - \overline{r}_{v,m}) \cdot \overline{\Phi}_k), \qquad (2)$$

where $\boldsymbol{w} = [w_1, ..., w_K]^T$ is a power weighting vector to be optimized. $\overline{\Phi}_k$ is a unit position vector of the kth probe.

To minimize the emulation error over M location pairs, the following objective function is used:

$$\min_{\boldsymbol{w}} \ \|\mathbf{F}_S \boldsymbol{w} - \boldsymbol{\rho}\|_2^2, \qquad (3)$$
$$\text{s.t. } 0 \le w_k \le 1, \ \forall k \in [1, K]$$

where $\mathbf{F}_S \boldsymbol{w} = \hat{\boldsymbol{\rho}}$ and $\boldsymbol{\rho}$ are the emulated spatial correlation and target spatial correlation vectors of size M, respectively, with the mth element corresponding to the spatial correlation between two isotropic antennas at the mth location pair. The M location pairs are selected on the surface of the test volume, as in [11]. Other ways to select location pairs, e.g. throughout the test volume, might give better emulation accuracy. However, they are not considered in this paper due to the computation complexity. $\mathbf{F}_S \in \mathbb{C}^{M \times K}$ is the transfer matrix whose elements are, according to (2), given by:

$$(\mathbf{F}_S)_{m,k} = \exp(ja(\overline{r}_{u,m} - \overline{r}_{v,m}) \cdot \overline{\Phi}_k), \quad 1 \le m \le M \qquad (4)$$

B. Plane wave synthesis (PWS)

Two channel modeling schemes based on the PWS techniques have been proposed in the literature as summarized below:

- In one channel modeling scheme [2], [3], a channel with a given incoming SPS is modeled by a collection of plane waves. Each of the plane waves impinging the test area with a specific angle-of-arrival can be approximated by allocating appropriate complex weights to the probes. The weights are obtained using optimization techniques, e.g. least mean square. A Doppler shift can then be introduced to each static plane wave to enable time variant channels.

This article has been accepted for publication in a future issue of this journal, but has not been fully edited. Content may change prior to final publication. Citation information: DOI 10.1109/TAP.2014.2301179, IEEE Transactions on Antennas and Propagation

Note that the complex weights to create each of the plane waves have to be determined only once and the temporal behavior is generated by multiplying the fixed weight with a rotating phasor. Also note that this is essentially a stationary channel model with fixed angles of arrival, as the incoming SPS has a specified shape.

- In another channel modeling scheme proposed in [4], each snapshot of the time-varying channel is considered static. The snapshots are characterized by the angles-of-arrivals, complex amplitudes, and polarizations of all waves, and hence can be reproduced by allocating appropriate complex weights to the multiple probes. The static plane waves are approximated from the spherical wave theory point of view. Arbitrary multipath environments (e.g. channels with time-varying angles of arrival) can be reproduced using this channel modeling scheme, unlike the first method. Note that the complex weights are calculated for each snapshot of the channel.

The basis for both channel modeling schemes is to obtain optimal complex weights for creating static plane waves with arbitrary angles-of arrivals for θ and φ polarizations. Note that same notations as [2] have been adopted in this paper. In order to ensure the emulated field approximates the target field in terms of magnitude, phase and polarization for all the samples inside the test volume, decomposition into three orthogonal axes x, y and z is required. The weighting vector $\boldsymbol{g_\theta}$ for a θ polarized plane wave can be obtained by solving the optimization problem as follows:

$$\min_{\mathbf{g}_{\boldsymbol{\theta}}} \left\| \begin{bmatrix} \mathbf{F}_{\theta,x} \\ \mathbf{F}_{\theta,y} \\ \mathbf{F}_{\theta,z} \end{bmatrix} \boldsymbol{g_\theta} - \begin{bmatrix} \boldsymbol{t}_{\theta,x} \\ \boldsymbol{t}_{\theta,y} \\ \boldsymbol{t}_{\theta,z} \end{bmatrix} \right\|_2^2 \quad \text{s.t. } 0 \le |g_{\theta,k}| \le 1 \; \forall k \in [1,K] \tag{5}$$

where

- $\mathbf{g}_{\boldsymbol{\theta}} = \{g_{\theta,k}\} \in \mathbb{C}^{K\times 1}$ is a vector of the complex weights for θ polarized probes.
- $\boldsymbol{t}_{\theta,x}$, $\boldsymbol{t}_{\theta,y}$, and $\boldsymbol{t}_{\theta,z} \in \mathbb{C}^{M\times 1}$ are vectors of θ polarized complex target fields projected to the x, y and z axes, respectively. M is the total number of samples.
- $\mathbf{F}_{\theta,x}$, $\mathbf{F}_{\theta,y}$ and $\mathbf{F}_{\theta,z} \in \mathbb{C}^{M\times K}$ are transfer matrices of known field propagation coefficients from the K probes to the M sample points for the θ polarization projected to the x, y and z axes, respectively.

The same principle can be applied for the φ polarization.

III. Probe selection algorithm

A. General formulation

Without the explicit constraints for each element of the weighting vector, the objective functions (3) and (5) can be written in a generic format as:

$$\min_{\mathbf{c}} \|\mathbf{F}\mathbf{c} - \boldsymbol{t}\|_2^2 \tag{6}$$

where $\mathbf{F}$ and $\boldsymbol{t} \in \mathbb{C}^{\boldsymbol{M\times 1}}$ are the transfer matrix and the target as specified in Sec. II. $\boldsymbol{c} = [c_1, ..., c_K]$ is the weighting vector to be optimized for the K probes. Note that the constraint for $\boldsymbol{c}$ is different for the PWS and the PFS technique. All the constraints documented in the previous section are convex constraints. Therefore, the formulation in (6) with additional convex constraints is a convex problem in this study. For simplicity, the constraints are omitted in the following problem formulation for the probe selection.

Then, the objective of the probe selection is to reproduce the channel models in the test volume with N OTA probes selected from the available K probes, i.e. to select N probes for channel emulation and disconnect the remaining probes from the channel emulator. The problem formulation for the probe selection is as follows:

$$\min_{\mathbf{c}} \; \|\mathbf{F}\mathbf{c} - \boldsymbol{t}\|_2^2 \quad \text{s.t. } \|\mathbf{c}\|_0 = N \tag{7}$$

where the norm-0 operation $\|\cdot\|_0$ is defined to be the number of nonzero entries in the vector. The problem in (7) is non-convex and NP-hard due to the norm-0 constraint.

After knowing locations of the nonzero entries, the optimization is simplified to be a convex optimization problem as:

$$\min_{\mathbf{c}_{sel}} \|\mathbf{F}_{sel}\mathbf{c}_{sel} - \boldsymbol{t}\|_2^2$$

where $\mathbf{F}_{sel}$ is the $M \times N$ matrix with N selected columns from $\mathbf{F}$, and $\mathbf{c}_{sel}$ is the $N \times 1$ vector with N selected probe locations.

B. Probe selection for the single cluster and multi-cluster channels

The concept of clusters has been widely adopted to model the multipath phenomenon based on extensive measurements. The radio waves could gather in one cluster or several clusters distributed over the space domain, see e.g. the SCME models [22]. Different clusters have different delays, thus making the channel wideband. Single cluster channel models and multi-cluster channel models have to be treated in a different manner in the probe selection process. In order to preserve the delay information of the channel, each cluster should be emulated individually with the multiple probes [21]. However, this is problematic with the probe selections. If each cluster is emulated independently, different sets of probes may be selected for different clusters, and the total number of selected probes might be larger than the number of available channel emulator output ports.

We propose to perform one probe selection optimization for the combined clusters, i.e. without delay discrimination and thus essentially a narrowband channel, instead of performing a probe selection optimization for each cluster. After knowing N probes for the narrow-band multi-cluster channel models, each cluster of the wideband channel can be then emulated individually with the same selected N probes.

C. Probe selection for different channel modeling schemes based on PWS technique: angular static and dynamic

If the target channel model consists of only static plane waves, the target field will be the sum of the static fields.

This article has been accepted for publication in a future issue of this journal, but has not been fully edited. Content may change prior to final publication. Citation information: DOI 10.1109/TAP.2014.2301179, IEEE Transactions on Antennas and Propagation

The probe selection process can be directly applied. For time varying channels modeled with the two channel modeling schemes based on the PWS techniques mentioned in Sec.II-B, two different probe selection processes should be considered.

- For channels emulated with the channel modeling scheme as described in [2], [3], the probe selection should be based on the SPS of the target channels, as the target is to form a channel with the target incoming SPS shape [2]. Hence the probe selection algorithm should be based on spatial correlation error. After selecting the optimal N probes for the target channel models, each of the different plane waves that are used to form the SPS is emulated individually with the same selected N probes. As explained in [2], complex weights for the PWS are function of angle-of-arrival of the plane wave and the probe configuration only. Even though the complex weights are time dependent for time-varying channels, the angle-of-arrival dependent part has to be determined only once. Temporal behavior is generated by multiplying the fixed weights with a rotating phasor. It is possible to precalculate the complex weights for each plane wave synthesis, which would reduce the computing time significantly during emulation.
- For channels emulated with channel modeling scheme detailed in [4], the time-varying channel at a time moment (each snapshot) can be represented by a collection of static plane waves. At each snapshot, since the target channel is static plane waves, the probe selection process can be directly applied. Different snapshots may present different target plane waves, and thus a different set of N probes might be selected for different snapshots of the channel. Note that probe switching from snapshot to snapshot is required, and the probe-switching time has to be shorter than the required channel update rate.

D. Probe selection algorithms

Different probe selection algorithms are detailed in the following part to deal with the non-convex problem explained in (7). As a benchmark, we perform the channel emulation with all the available K probes to evaluate the performance deterioration when less probes are used. This channel emulation with all available probes can be simply treated as a performance upper bound. It worth mentioning here that the probe selection algorithm is similar to the antenna selection process in MIMO communication systems [23], [24].

1) Brute force algorithm: A straightforward way to select probes is to use the brute force method where the optimization is performed for each possible combination of the N probes out of K probes. Then weights which result in the best fit in terms of spatial correlation accuracy or field synthesis accuracy using N probes will be selected. Therefore, the total number of combinations is $\begin{pmatrix} K \\ N \end{pmatrix}$. When we go over all the possible combinations, the combination which gives the minimum emulation error can be obtained. However, the number of combinations to be tested becomes huge when K is large. Other alternatives have to be considered as the computation time for the probe selection is crucial.

Algorithm 1 Multi-shot algorithm

Set $n = 0$ and $k_0 = 0$

Iterate

Update $n = n + 1$ until $K - \sum_{m=0}^{n-1} k_m = N$

1. Build $\mathbf{F}_n$ based on $K - \sum_{m=0}^{n-1} k_m$ active probes
2. Optimize for $K - \sum_{m=0}^{n-1} k_m$ active probes

$$\min_{\mathbf{c}_n} \|\mathbf{F}_n \mathbf{c}_n - \boldsymbol{t}\|_2^2 .$$

3. In $\mathbf{c}_n$, remove k_n probes with least power values.

Return $N \times 1$ vector $\mathbf{c}_n$ based on $\min_{\mathbf{c}_n} \|\mathbf{F}_n \mathbf{c}_n - \boldsymbol{t}\|_2^2$ and the corresponding N probe index numbers

2) Multi-shot algorithm: Alternatively, probes can be selected in a sequential manner in the multi-shot algorithm. In this multi-shot algorithm, we will remove a certain number of probes at each iteration ("shot"). Basically, in each iteration the probes with least contributions are removed. Note that the number of probes removed in each iteration is not necessarily constant. We denote by k_n the number of probes we remove in the nth iteration and $\mathbf{F}_n$ is the matrix associated with the selected $K - \sum_{m=0}^{n-1} k_m$ probes in the nth iteration.

In the multi-shot algorithm, we first perform the power optimization for K probes. In the nth iteration, based on the individual probe power values in $\mathbf{c}_n$, we remove k_n probes with the least contributions. We repeat the probe removal process until only $K - \sum_{m=0}^{n-1} k_m = N$ probes are left. In the end, we return both the final probe weights and the corresponding probe index numbers. The detailed process is summarized in Algorithm 1.

3) Successive probe cancellation (SPC) algorithm: In the multi-shot algorithm, we are removing probes with least power values and form a new optimization with less probes in an iterative manner. In contrast, for the SPC algorithm we select probes with largest power values in a sequentially manner. This probe selection algorithm adopts the idea of successive interference cancellation (SIC) technique, which is a popular technique in wireless communications.

The key idea is to find the probes with most contributions in each iteration. Then the contributions of the selected dominant probes are removed in the target and the consequent probe power optimizations. In each iteration, we target to find a certain number of dominant probes and the number of probes selected does not need to remain the same across the iterations.

In this algorithm, we still perform the probe power optimization for K probes at first. In each iteration, we will select a certain number of active probes with largest power contributions and store the probe index numbers and the corresponding angular locations. To differentiate from the k_n used in the multi-shot algorithm, we denote p_n to be the number of probes we select in the nth iteration and $\mathbf{F}_n$ to be the matrix associated with the remaining non-selected $K - \sum_{m=0}^{n-1} p_m$ probes in the nth iteration. In the beginning of each iteration, we update $\mathbf{F}_n$ according to the current remaining non-selected probes. Then to prepare for the subsequent optimization, we remove the contributions of the selected probes by modifying the target $\boldsymbol{t}_{n+1} = \boldsymbol{t}_n - \mathbf{F}_n \hat{\mathbf{c}}_n$, where $\hat{\mathbf{c}}_n$ is the weighting

This article has been accepted for publication in a future issue of this journal, but has not been fully edited. Content may change prior to final publication. Citation information: DOI 10.1109/TAP.2014.2301179, IEEE Transactions on Antennas and Propagation

Algorithm 2 Successive probe cancellation (SPC) algorithm

Set $n = 0$ and $p_0 = 0$

Iterate

Update $n = n + 1$ until $\sum_{m=0}^{n-1} p_m = N$

1. Build $\mathbf{F}_n$: $K - \sum_{m=0}^{n-1} p_m$ non-selected probes
2. Optimize for $K - \sum_{m=0}^{n-1} p_m$ active probes

$$\min_{\mathbf{c}_n} \|\mathbf{F}_n \mathbf{c}_n - \boldsymbol{t}_n\|_2^2 .$$

3. Select p_n probes with largest power values in $\mathbf{c}_n$
4. Compute $\hat{\mathbf{c}}_n$ and update $\boldsymbol{t}_{n+1} = \boldsymbol{t}_n - \mathbf{F}_n \hat{\mathbf{c}}_n$

Return the selected N probe index numbers and derive the power weights based on $\min_{\mathbf{c}_{spc}} \|\mathbf{F}_{spc}\mathbf{c}_{spc} - \boldsymbol{t}\|_2^2$

vector obtained from $\mathbf{c}_n$, and $\hat{\mathbf{c}}_n$ consists of the weights for the p_n selected probes from $\mathbf{c}_n$ in the nth iteration and the rest entries set to zero. This probe contribution cancellation process carried out in the end of each iteration, is analogous to the SIC technique. We continue the iteration until $\sum_{m=0}^{n-1} p_m = N$ probes are selected. In the end, based on the selected probes, we build $\mathbf{F}_{spc}$ and perform a final optimization to find the power weights $\mathbf{c}_{spc}$. The successive probe cancellation (SPC) algorithm is detailed in Algorithm 2.

The main difference from the multi-shot algorithm lies in that the contributions of the removed probes are also removed from the target, whereas in the multi-shot algorithm the target stays the same throughout all the iterations.

4) One-shot algorithm: A simple way to select probes is to use the one-shot method where the convex optimization is performed with K probes for $\min_{\mathbf{c}} \|\mathbf{F}\mathbf{c} - \boldsymbol{t}\|_2^2$. Based on the individual probe power values $|c_{index}|$ $(1 \leq index \leq K)$, $(K - N)$ probes with least power values are removed.

We denote $\mathbf{F}_{one}$ to be the matrix associated with the selected N probes of dimension $M \times N$. Then we perform the optimization for the remaining N probes with $\mathbf{c}_{one}$ being the $N \times 1$ vector

$$\min_{\mathbf{c}_{one}} \|\mathbf{F}_{one}\mathbf{c}_{one} - \boldsymbol{t}\|_2^2 .$$

5) Algorithm Summary: In the multi-shot algorithm, we can remove different number of probes in each iteration, $k_n \neq k_m \, (m \neq n)$. If we set $k_n = k_m = k \, (m \neq n)$, we need to apply the convex optimization $\frac{K-N}{k} + 1$ times to accomplish the probe selection process. The previous one-shot algorithm is an extreme case of the multi-shot algorithm where $k = K - N$ is used. Also, if we set $p_n = p_m = p \, (m \neq n)$ for the SPC algorithm, we need to apply the convex optimization $\frac{N}{p} + 1$ times. Notice that the one-shot algorithm is also an extreme case of the SPC algorithm where $p = N$ is used. A summary of different algorithms is given in Table I.

As described above, different k_m and p_m can be used in simulations. In the following numerical evaluations, $k_n = k_m = 1 \, (m \neq n)$ and $p_n = p_m = 1 \, (m \neq n)$ are chosen for the multi-shot algorithm and the SPC algorithm, unless otherwise stated. Further investigations are needed to find the tradeoff between computation complexity and accuracy for various target channel models and probe configurations.

Table I
ALGORITHM COMPARISON (SELECTION: N OF K PROBES)

Algorithm	Number of convex optimizations	Emulation performance
Brute force	$\binom{K}{N} = \frac{K!}{(K-N)!N!}$	Best performance
One-shot	2	Worst performance
Multi-shot	$\frac{K-N}{k} + 1$	No worse than one-shot
Successive probe cancellation	$\frac{N}{p} + 1$	No worse than one-shot
No probe selection (benchmark)	1	Performance bound

Table II
PROBE CONFIGURATIONS. ($K = 48$)

Case	Probe Setup
P1	$\theta_1 = -30^o \ \phi_{1i} = -180^o + i \cdot 30^o, i \in [1, ..., 12]$
	$\theta_2 = 0^o \ \phi_{2i} = -180^o + i \cdot 15^o, i \in [1, ..., 24]$
	$\theta_3 = 30^o \ \phi_{3i} = -180^o + i \cdot 30^o, i \in [1, ..., 12]$
P2	$\theta_1 = -45^o \ \phi_{1i} = -180^o + i \cdot 45^o, i \in [1, ..., 8]$
	$\theta_2 = -10^o \ \phi_{2i} = -180^o + i \cdot 22.5^o, i \in [1, ..., 16]$
	$\theta_3 = 10^o \ \phi_{3i} = -180^o + i \cdot 22.5^o, i \in [1, ..., 16]$
	$\theta_4 = 45^o \ \phi_{4i} = -180^o + i \cdot 45^o, i \in [1, ..., 8]$

IV. SIMULATION RESULTS

The probe configurations and the target channel models are firstly described in this part. After that, the simulation results with different probe selection algorithms are shown. The total number of available probes is $K = 48$, and the number of output ports of the channel emulator N is set to 16. The test volume size is selected to be one wavelength. Vertical polarization is assumed for all the target channel models, for the sake of simplicity.

A. Probe configuration

Two different probe configurations are assessed for the probe selection algorithm, as detailed in Table II. The probes are placed on a sphere, and the elevation angle θ and the azimuth angle φ are specified for each probe. The probes are organized on several elevation rings. θ_l denotes the elevation angle for all the probes on the lth elevation ring. ϕ_{lj} is the azimuth angle of the jth probe on the lth elevation ring. Figure 2(a) and Figure 2(b) illustrate the probe configuration P1 and P2, respectively.

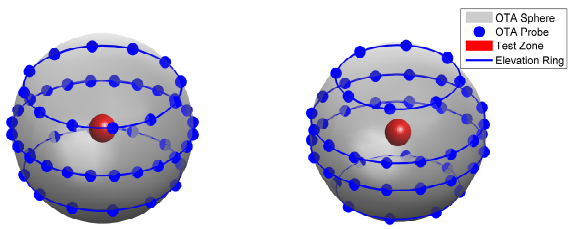

(a) Probe setup P1 (b) Probe setup P2

Figure 2. An illustration of probe configuration P1 (a) and P2 (b), detailed in Table II.

This article has been accepted for publication in a future issue of this journal, but has not been fully edited. Content may change prior to final publication. Citation information: DOI 10.1109/TAP.2014.2301179, IEEE Transactions on Antennas and Propagation

Table III
TARGET SINGLE CLUSTERS

Target Case	Target Spherical Power Spectrum		
	PAS shape	PES shape	Comment
A	AoA = 0^o ASA = 35^o	EoA = 0^o ESA = 10^o	Laplacian shaped PAS and PES, as shown in Figure 4
B	AoA = 15^o ASA = 35^o	EoA = 15^o ESA = 10^o	Gaussian shaped PAS and PES
C	Uniform	EoA = 0^o ESA = 10^o	Uniform shaped PAS and Laplacian shaped PES, as shown in Figure 3

Table IV
TEST CASE D FOR THE ALGORITHM COMPARISON

Cluster Index	Cluster info	1	2	3	4	5	6
PAS	AoA [^{o}]	66	46	143	33	-91	-19
	ASA [^{o}]	35	35	35	35	35	35
PES	EoA [^{o}]	0	-10	0	10	0	15
	ESA [^{o}]	10	10	10	10	10	10
Power [dB]		0	-2.2	-1.7	-5.2	-9.1	-12.5

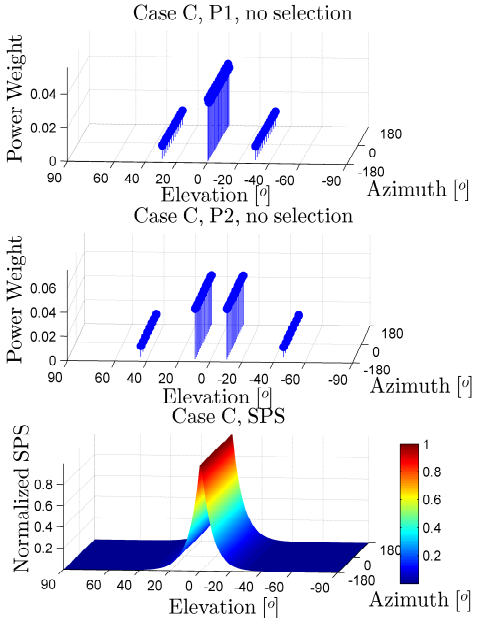

Figure 3. Emulated and target SPS for case C and using all probes for the two probe configurations.

B. Probe selection simulation results for the PFS technique

Three target single cluster channel models are considered, as detailed in Table III. The SPS is modeled independently by the power azimuth spectrum (PAS) characterized by the azimuth angle of arrival (AoA) and azimuth spread of arrival (ASA), and the power elevation spectrum (PES) characterized by the elevation angle of arrival (EoA) and elevation spread of arrival (ESA) [15]. Several different PAS and PES models are considered for the target channel models. A multi-cluster channel model is considered as well, as described in Table IV. The considered model is the SCME UMa TDL model extended to 3D. The SCME models are defined only on the azimuth plane and with no spread over the elevation dimension. Here a Laplacian shaped PES is introduced to each of the clusters. Note that the proposed algorithms are not restricted to any model, and SPS based on measurements can be reproduced as well.

Figure 3 and Figure 4 shows the emulated and target SPS for target channel case C with no probe selection and case A with the one-shot algorithm, respectively. As discussed previously, the emulated discrete SPS is characterized by power weights of the probes. The shape of the emulated discrete SPSs match well visually with the shape of the continuous target PASs for both cases. The target SPS for case D is shown in Figure 5 (below). As we can see in Figure 5 (top), no probes corresponding to the 5th and 6th cluster are selected, as the probe selection optimization is based on the SPS of the multi-cluster model (without delay discrimination). The selected probes are favoring the dominant clusters, so the emulation accuracy for individual clusters might be bad. The target spatial correlation $|\rho|$ for case D and associated correlation error $|\rho - \hat{\rho}|$ associated with no probe selection, the one-shot and the multi-shot algorithm are shown in Figure 6. The spatial correlation between the antennas u and v varies with the location pair position. The distance between the location pair is the test volume size, i.e. 1λ, and the location pair position is characterized by the elevation and azimuth angle.

The root mean square (RMS) values of the correlation error $|\rho-\hat{\rho}|$ with different algorithms for the considered target channel models are shown in Table IV-B. The deviation between the theoretical spatial correlation of the target continuous SPS, and the emulated correlation of the discrete SPS depends on the channel models and probe configurations. Note that generally the correlation error $|\rho-\hat{\rho}|$ increases as we increase the test volume size [2], [11], [21]. That is, the correlation error with antenna separation smaller than test volume size will be smaller than the values presented in Table IV-B.

The performance deterioration when less probes are used is quite small for case A, case C and case D, which is expected as the cluster is arriving to the test zone from the direction where the probes are located. For case B, the emulation accuracy is worse as the cluster is impinging from an angle between the probes. The no probe selection case provides the best emulation accuracy for all the cases, as expected. The one-shot algorithm provides slightly worse or the same performance as the multi-shot algorithm, as all the probes with high weights are selected both for the one-shot algorithm and the multi-shot algorithm, and only a few probes with small weights are selected differently, as shown in Figure 5 and Figure 6 for case D, as an example. The same probes are selected for the one-shot algorithm and the SPC algorithm for all the considered scenarios. All the proposed probe selection algorithms work well, as the correlation error is only slightly worse than the case with no probe selection.

The RMS of the correlation error $|\rho - \hat{\rho}|$ as a function of number of selected probes for the two probe configurations with the one-shot and the multi-shot algorithm is shown in Figure 7. The more probes selected, the better channel emulation accuracy we can achieve for all scenarios, as expected. This improvement, however, saturates at a certain number

This article has been accepted for publication in a future issue of this journal, but has not been fully edited. Content may change prior to final publication. Citation information: DOI 10.1109/TAP.2014.2301179, IEEE Transactions on Antennas and Propagation

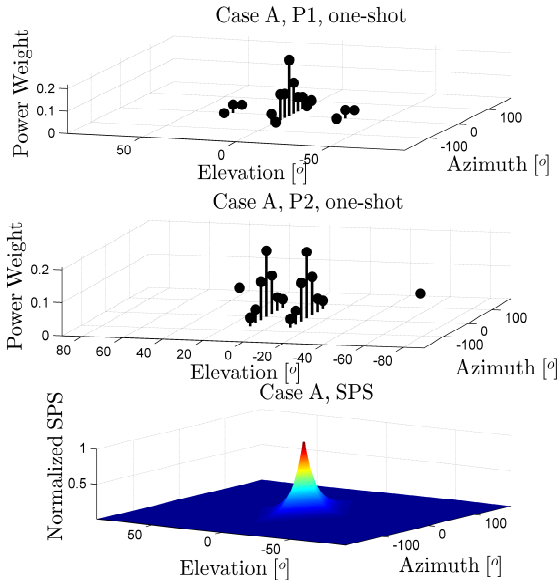

Figure 4. Emulated and target SPS for case A with the one-shot algorithm for the two probe configurations.

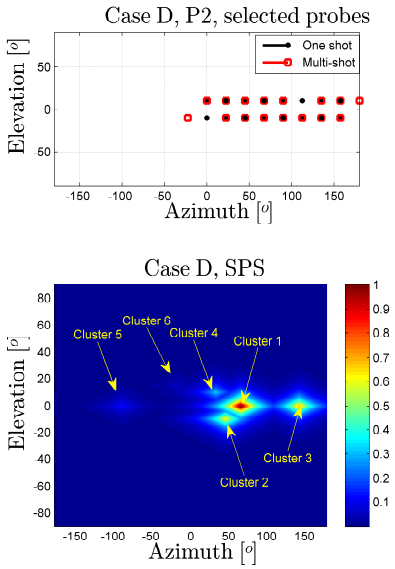

Figure 5. The target SPS and selected probes with the one-shot and the multi-shot algorithm for case D.

Table V
RMS OF THE EMULATION ERROR $|\rho - \hat{\rho}|$ WITH DIFFERENT ALGORITHMS FOR DIFFERENT TARGET MODELS. $N = 16$

Method	Probe Setup	A	B	C	D
No probe selection	P1	0.028	0.278	0.018	0.019
	P2	0.047	0.16	0.025	0.009
One-shot	P1	0.031	0.281	0.029	0.024
	P2	0.06	0.16	0.061	0.023
Multi-shot	P1	0.03	0.28	0.029	0.023
	P2	0.057	0.16	0.036	0.02
SPC	P1	0.031	0.281	0.029	0.024
	P2	0.06	0.16	0.061	0.023

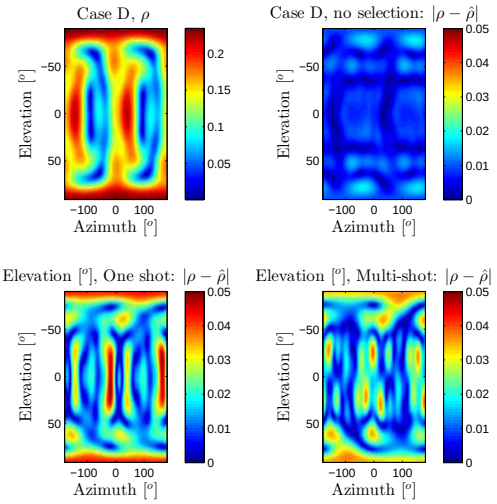

Figure 6. The target spatial correlation $|\rho|$ and the associated correlation error $|\rho - \hat{\rho}|$ with no probe selection, the one-shot and the multi-shot algorithm for case D.

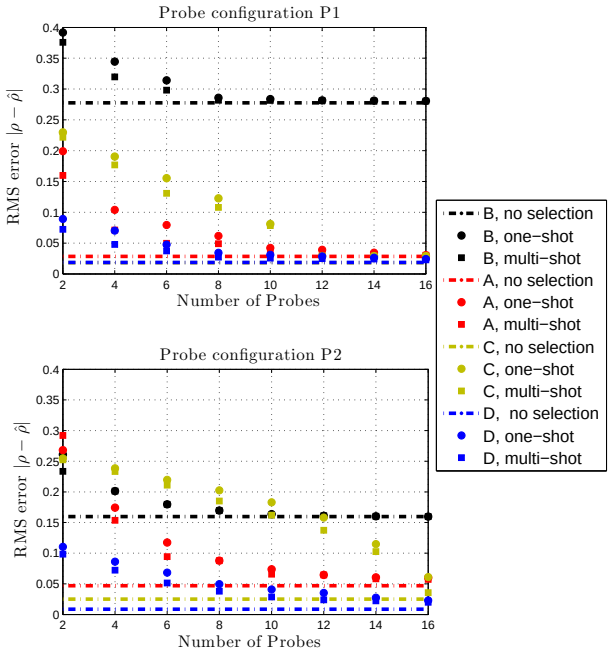

Figure 7. The RMS error $|\rho - \hat{\rho}|$ as a function of the number of selected probes for the two probe configurations. Note that for probe configuration P1, the curve with no probe selection for channel model C is on top of the curve with no probe selection for channel model D.

of selected probes, depending on the target channel models and probe configuration. The multi-shot algorithm generally outperforms, though marginally, the one-shot algorithm. This is due to the fact that only a few probes with small weights are selected differently in the two algorithms.

C. Probe selection for the PWS technique

As explained in Section II-B, the basis for radio channel emulation with the PWS techniques is to reproduce the static plane waves. Three static scenarios are considered as examples

This article has been accepted for publication in a future issue of this journal, but has not been fully edited. Content may change prior to final publication. Citation information: DOI 10.1109/TAP.2014.2301179, IEEE Transactions on Antennas and Propagation

Table VI
TARGET STATIC PLANE WAVES

Target case	E	F	G
AoA [^{o}]	0	100	Two static plane waves detailed in case E and F, respectively.
EoA [^{o}]	0	15	
Target field at test volume	Phase 0^o at center		
	Uniform magnitude of 1 over test volume		
Comment	Vertically polarized	Vertically polarized	

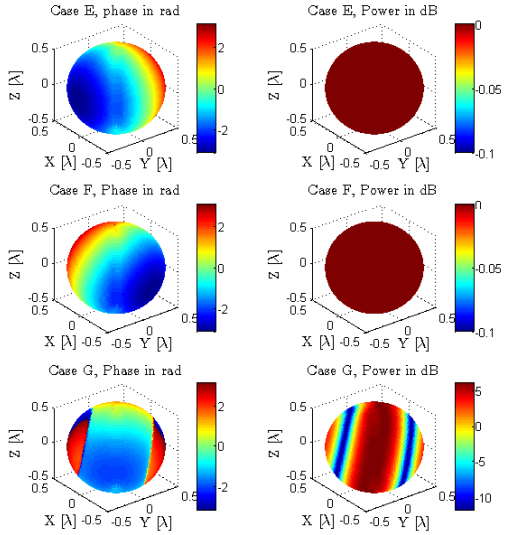

Figure 8. The phase and power distribution over test volume of target scenario E (top), F (middle) and G (bottom), respectively.

for the target scenarios, as detailed in Table VI. The impinging angle of each plane wave is characterized by the AoA and EoA. A single static plane wave is considered in case E and in case F, respectively. Case F represents a critical scenario where the target plane wave is impinging from between the probes, while case E is expected to offer better emulation accuracy. A multi-static plane wave case is considered in case G. Figure 8 illustrates the phase and power distribution over the test volume of target scenario E, F, and G, respectively. Linear phase fronts along the propagation direction and uniform power distribution over the test volume can be observed for scenario E and F. For scenario G, the fades in power are caused by the destructive superposition of two static plane waves with different propagation directions. To characterize the deviation between the target field and synthesized field, the maximum of the error vector magnitude in dB among all the sample points on the surface of the test volume ϵ is defined as follows:

$$\epsilon = \max\{10\lg(|\mathbf{F}_{\xi,x}\boldsymbol{g}_{\boldsymbol{\xi}} - \boldsymbol{t}_{\xi,x}|^2 + |\mathbf{F}_{\xi,y}\boldsymbol{g}_{\boldsymbol{\xi}} - \boldsymbol{t}_{\xi,y}|^2 + |\mathbf{F}_{\xi,z}\boldsymbol{g}_{\boldsymbol{\xi}} - \boldsymbol{t}_{\xi,z}|^2)\},$$

where ξ denotes either θ or φ polarization. The maximization is performed over M sample points.

A summary of field synthesis error ϵ with different algorithms is shown in Table VII. The polarization of the target

Table VII
FIELD SYNTHESIS ERROR ϵ [dB] WITH DIFFERENT ALGORITHMS. N = 16

Method	Probe Setup	E	F	G
No probe selection	P1	-28.72	-13.28	-13
	P2	-23.1	-22.1	-20.2
One-shot/SPC	P1	-28.58	-13.39	-9.95
	P2	-22.31	-21.24	-19.23
Multi-shot	P1	-28.57	-13.31	-9.96
	P2	-22.30	-21.11	-19.17

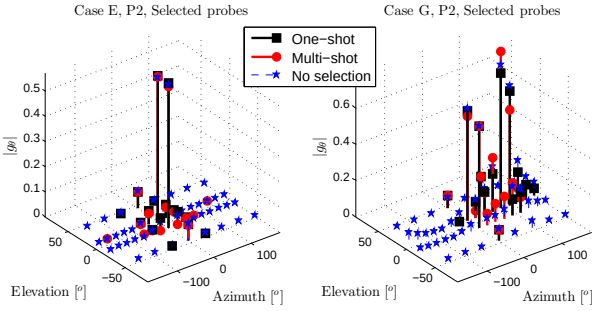

Figure 9. Magnitude of the complex weights for the selected probes with the one-shot and the multi-shot algorithm for case E (left) and case G, respectively.

channel models E, F, and G are detailed in Table VI. The same probes are selected for the SPC algorithm as the one-shot algorithm and the results are not shown. ϵ depends on the target channel models and probe configurations, as previously discussed. The performance deterioration when less probes are used is marginal. This is due to the fact that only a few probes are dominant when synthesizing the target channel models, as shown in Figure 9, for example. Also, as all the probes with high weights are selected both for the one-shot algorithm and the multi-shot algorithm, the two probe selection algorithms present similar performance.

D. A critical probe configuration for the one-shot algorithm

In the previously considered cases, the one-shot algorithm presents only slightly worse results than the multi-shot algorithm. This is due to the fact that the number of selected probes N is sufficiently large that all dominant probes are selected with the one-shot and the multi-shot algorithm. To better demonstrate the difference between the two algorithms for the scenarios where the number of selected probes N is smaller than the number of dominant probes, a simple 2D probe configuration and a 2D target channel model are considered, as detailed in Table VIII. Note this probe configuration with $K = 360$ might be practically unrealistic due to the issues such as the power coupling between probes, reflections and physical size. This case is included only to illustrate the problems with the one-shot algorithms.

The target spatial correlation $|\rho|$ and the associated emulated spatial correlation $|\hat{\rho}|$ with no probe selection, the multi-shot algorithm and the one-shot algorithm with $N = 5$ for the case H is shown in Figure 10 (top). As we can see, the multi-shot algorithm works well and the correlation error $|\rho - \hat{\rho}|$ is quite small. However, the one-shot algorithm presents

This article has been accepted for publication in a future issue of this journal, but has not been fully edited. Content may change prior to final publication. Citation information: DOI 10.1109/TAP.2014.2301179, IEEE Transactions on Antennas and Propagation

Table VIII
A CRITICAL PROBE CONFIGURATION.

Target Channel Case:H	Probe configuration P3	Test area size
Laplacian shaped PAS with AoA = 22.5^o and ASA = 35^o	$K = 360$ uniformly distributed probes on the azimuth plane	0.7λ

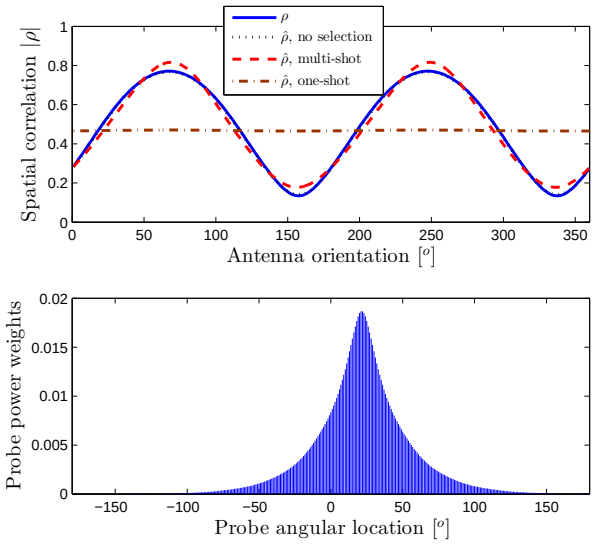

Figure 10. The target spatial correlation $|\rho|$ and the associated emulated spatial correlation $|\hat{\rho}|$ with no probe selection, the multi-shot and the one-shot algorithms for case H (top). The probe weights with no probe selection is shown in the figure as well (bottom). The selected number of probes is $N = 5$.

large deviations. The probe weights for the probes selected with the one-shot algorithm and the multi-shot algorithm are shown in Figure 11. The probes around AoA = 22.5^o are selected for the one-shot algorithm, as the probes with high weights concentrate around AoA = 22.5^o, as shown in the Figure 10 (bottom). However, these selected probes will be incapable of creating the azimuth spread of target channels. The power weights of the $N = 5$ selected probes are shown in Figure 11 (left). The zeros for the middle probes are due to the convex optimization after the probe selection. As the optimization attempts to create the azimuth spread of the channel, effectively only two probes with larger angular distance to AoA = 22.5^o are used to synthesize the channel. With the multi-shot algorithm, the emulated PAS follows well the target PAS, as shown in the Figure 11 (right).

The RMS error $|\rho - \hat{\rho}|$ as a function of the number of selected probes for the target channel H with the one-shot and the multi-shot algorithm is shown in Figure 12. The multi-shot algorithm clearly outperforms the one-shot algorithm. The SPC algorithm presents the same results as the one-shot algorithm, as the same probes are always selected.

V. MEASUREMENT VERIFICATION

A measurement campaign was carried out in a practical setup at Aalborg University to verify the proposed probe

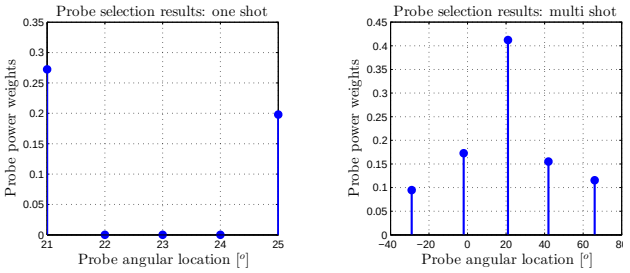

Figure 11. The probe weights for the probes selected with the one-shot algorithm (left) and the multi-shot algorithm (right) with $N = 5$.

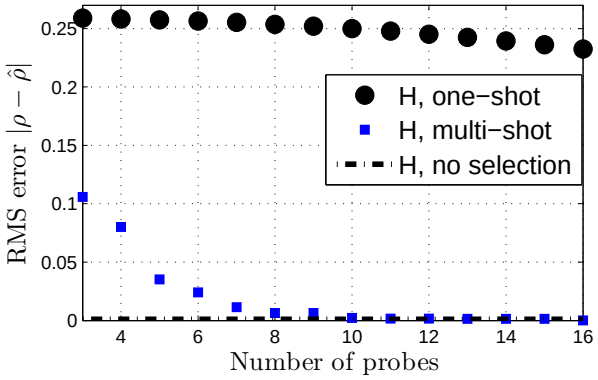

Figure 12. The RMS error $|\rho - \hat{\rho}|$ as a function of number of selected probes for target channel H with the probe configuration P3.

selection algorithm. Figure 13 shows the practical multi-probe setup inside the anechoic chamber. A small choke is used on the test dipole to minimize cable effects. The measurement setup and the spatial correlation measurement procedure were described in section IV of [21] and not detailed here. A summary of the measurement setup is given in Table IX. As detailed in Table X, three test cases are considered for the measurement campaign. The total available number of probes is $K = 16$ and the number of selected probes is $N = 8$. It is desirable that with the selected subset of probes ($N = 8$), we can emulate the SCME UMi TDL model with comparable channel emulation accuracy achieved with 16 uniformly placed probes (i.e. with no probe selection). The multi-shot algorithm is used to select the subset of probes. Figure 14 illustrates the probe configurations for the three cases. The angular locations of the selected probes match well with the AoAs of the SCME UMa TDL model, as expected.

In [2], it is concluded that both channel emulation techniques are capable of creating spatial radio channel characteristics according to the target model. However, the PWS technique requires accurate phase calibration of the setup and hence the PFS technique is considered for the channel emulation in the measurements.

The simulation results of the spatial correlation $|\rho|$ for the SCME UMi TDL model and correlation error $|\hat{\rho} - \rho|$ with the three setups are shown in Figure 15. The radius d and polar angle ϕ_a of each point on the plots correspond to the value at antenna separation d and antenna orientation ϕ_a [21]. Given the error criteria $|\hat{\rho} - \rho|$, the corresponding radius of the

This article has been accepted for publication in a future issue of this journal, but has not been fully edited. Content may change prior to final publication. Citation information: DOI 10.1109/TAP.2014.2301179, IEEE Transactions on Antennas and Propagation

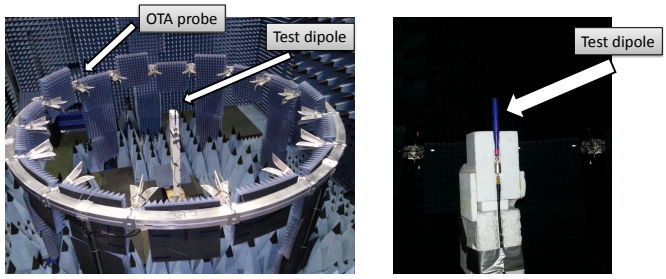

Figure 13. An illustration of the multi-probe setup (left) and the dipole setup (right) in the anechoic chamber.

Table IX
MEASUREMENT SETUP SUMMARY

	Setup and specifications
Target channel model	SCME urban micro (UMi) TDL model as detailed in [25] with carrier frequency $f_c = 1900$ MHz.
Test antenna	Satimo electric sleeve dipole at 1900MHz.
Test antenna position	25 test antenna positions sample a segment of line of length 24cm (around 1.5λ) with sampling interval of 1cm and with antenna orientation $\phi_a = 0^o$ and $\phi_a = 90^o$.
OTA probes	Three configurations as detailed in Table X and shown in Figure 14.

circle, which corresponds to the test area size, can be found. The antenna separation d and the antenna orientation ϕ_a are used to characterize the position of the location pair in 2D setup. Maximum deviation of 0.06 is achieved over the test area size of 1.5λ for the setup II with 16 probes. With 8 uniformly spaced probes, the test area is much smaller. With the setup III, a test area size of 1.5λ can be achieved with slight performance deterioration compared with setup II with 16 probes.

The target $|\rho|$, emulated $|\hat{\rho}|$ and measured $|\rho_{meas}|$ spatial correlation of the SCME UMi TDL model for the three setups for antenna orientation $\phi_a = 0^o$ and $\phi_a = 90^o$ are

Table X
TEST CASES FOR THE MEASUREMENTS

Setup	No. of Probe	Test area	probe configuration
I	8	0.7λ	uniformly spaced with 45^o angular separation
II	16	1.5λ	uniformly spaced with 22.5^o angular separation
III	8	1.5λ	8 probes selected from 16 uniformly placed probes

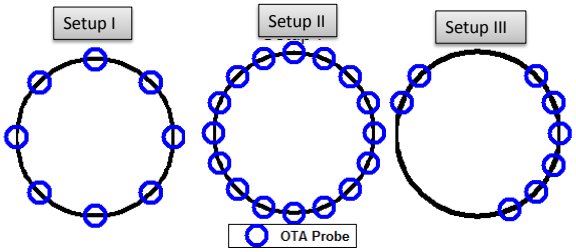

Figure 14. An illustration of the probe configurations for the three cases.

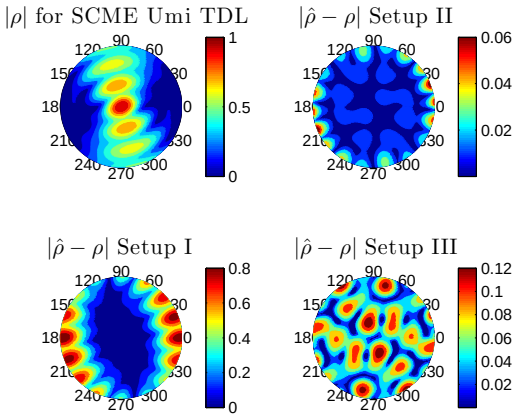

Figure 15. $|\rho|$ and spatial correlation error $|\rho - \hat{\rho}|$ for the SCME UMi TDL model for the three setups. Test area size: 1.5λ.

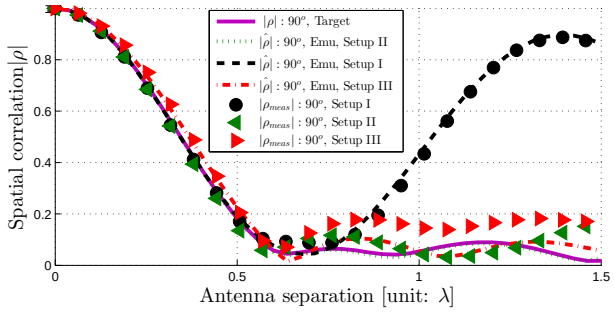

Figure 16. Comparison between target, emulated and measured spatial correlation for antenna orientation $\phi_a = 0^o$ for the three setups.

shown in Figure 16 and Figure 17, respectively. The deviations between $|\hat{\rho}|$ and $|\rho|$ depend on the probe configuration and the number of OTA probes [2], [21]. The measured spatial correlations $|\rho_{meas}|$ generally match well with the emulated spatial correlations $|\hat{\rho}|$ for the three setups.

The deviation caused by a difference between the plane and spherical waves due to the physical limitation of the OTA ring is negligible, according to the results in [26]. One possible reason for the deviation between measurements and simulations is that the radiation pattern of the test dipole presents around 1.5 dB variation due to the cable effect, although a small choke was used. As shown in the results, the channel emulation accuracy achieved with 8 selected probes is only slightly worse than that achieved with 16 uniformly placed probes.

VI. CONCLUSION

This paper presents three probe selection algorithms for 3D multi-probe based setups. The proposed techniques provide a probe selection framework for the two channel emulation techniques, i.e. the plane wave synthesis technique and the prefaded signal synthesis techniques. Simulation results show that good channel emulation accuracy can be achieved with the selected subset of probes for the considered target channel models. The one-shot algorithm presents lowest computation complexity and only slight performance deterioration compared with the multi-shot algorithm for the scenarios where

This article has been accepted for publication in a future issue of this journal, but has not been fully edited. Content may change prior to final publication. Citation information: DOI 10.1109/TAP.2014.2301179, IEEE Transactions on Antennas and Propagation

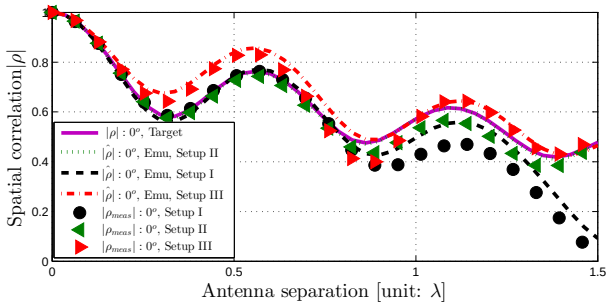

Figure 17. Comparison between target, emulated and measured spatial correlation for antenna orientation $\phi_a = 90^o$ for the three setups.

the number of selected probes is sufficiently large that all dominant probes are selected with the one-shot algorithm. For the scenarios where the number of selected probes is smaller than the number of dominant probes, the multi-shot algorithm generally outperforms the one-shot algorithm significantly. The probe selection algorithm for the SCME UMi TDL model is supported by measurements in a practical 2D multi-probe setup. The measurement results show that the channel emulation accuracy achieved with 8 selected probes is only slightly worse compared to that achieved with 16 uniformly placed probes for a test area of 1.5λ.

REFERENCES

[1] M. Rumney, R. Pirkl, M. H. Landmann, and D. A. Sanchez-Hernandez, "MIMO Over-The-Air Research, Development, and Testing," *International Journal of Antennas and Propagation*, vol. 2012, 2012.

[2] P. Kyösti, T. Jämsä, and J. Nuutinen, "Channel modelling for multiprobe over-the-air MIMO testing," *International Journal of Antennas and Propagation*, 2012.

[3] P. Kyösti, J. Nuutinen, and T. Laitinen, "Over the air test," Patent WO 2012/117 147 A1, Sep. 7, 2012.

[4] J. Toivanen, T. Laitinen, V. Kolmonen, and P. Vainikainen, "Reproduction of Arbitrary Multipath Environments in Laboratory Conditions," *Instrumentation and Measurement, IEEE Transactions on*, vol. 60, no. 1, pp. 275–281, 2011.

[5] P. Kyösti and J. Nuutinen, "Over the air test," Patent US 20 110 189 962, Aug. 4, 2011.

[6] J. D. Reed, "Emulation and controlled testing of MIMO OTA channels," Patent US 20 110 299 570, Dec. 8, 2011.

[7] W. Fan, X. Carren, J. Nielsen, K. Olesen, M. Knudsen, and G. Pedersen, "Measurement Verification of Plane Wave Synthesis Technique Based on Multi-Probe MIMO-OTA Setup," in *Vehicular Technology Conference (VTC Fall), 2012 IEEE*, 2012, pp. 1–5.

[8] W. Fan, X. Carreño, J. Ø. Nielsen, M. B. Knudsen, and G. F. Pedersen, "Channel Verification Results for the SCME models in a Multi-Probe Based MIMO OTA Setup," in *Vehicular Technology Conference (VTC Fall)*. IEEE, September 2013, pp. 1–5.

[9] S. Alessandro, F. C., and N. G., "MIMO OTA measurement with anechoic chamber method," in *Antennas and Propagation (EUCAP), 2013 7th European Conference on*. IEEE, April 2013.

[10] P. Kyosti, J.-P. Nuutinen, and T. Jamsa, "MIMO OTA test concept with experimental and simulated verification," in *Antennas and Propagation (EuCAP), Proceedings of the Fourth European Conference on*. IEEE, 2010, pp. 1–5.

[11] W. Fan, F. Sun, P. Kyösti, J. Nielsen, X. Carreño, M. Knudsen, and G. Pedersen, "3D channel emulation in multi-probe setup," *Electronics Letters*, vol. 49, pp. 623–625(2), April 2013.

[12] P. Kyösti and A. Khatun, "Probe Configurations for 3D MIMO Over-the-Air Testing," in *Antennas and Propagation (EUCAP), Proceedings of the 7th European Conference on*. IEEE, 2013.

[13] M. A. Mow, R. W. Schlub, and R. Caballero, "System for testing multi-antenna devices," Patent US 2011/0 084 887 A1, Apr. 14, 2011.

[14] T. Laitinen, P. Kyösti, J.-P. Nuutinen, and P. Vainikainen, "On the number of OTA antenna elements for plane-wave synthesis in a MIMO-OTA test system involving a circular antenna array," in *Antennas and Propagation (EuCAP), 2010 Proceedings of the Fourth European Conference on*. IEEE, 2010, pp. 1–5.

[15] M. B. Knudsen and G. F. Pedersen, "Spherical outdoor to indoor power spectrum model at the mobile terminal," *Selected Areas in Communications, IEEE Journal on*, vol. 20, no. 6, pp. 1156–1169, 2002.

[16] T. Taga, "Analysis for mean effective gain of mobile antennas in land mobile radio environments," *Vehicular Technology, IEEE Transactions on*, vol. 39, no. 2, pp. 117–131, 1990.

[17] "Spatial channel model for Multiple Input Multiple Output (MIMO) simulations (Release 11)," 3GPP/3GPP2, TR 25.996 V11.0.0, Sep. 2012.

[18] L. Hentilä, P. Kyösti, M. Käske, M. Narandzic, and M. Alatossava, "MATLAB implementation of the WINNER Phase II Channel Model ver1. 1," 2007.

[19] P. Kyösti, J. Nuutinen, and J. Malm, "Over the air test," Patent US 20 130 059 545 A1, Mar. 7, 2013.

[20] A. Khatun, H. Laitinen, V.-M. Kolmonen, and P. Vainikainen, "Dependence of Error Level on the Number of Probes in Over-the-Air Multiprobe Test Systems," *International Journal of Antennas and Propagation*, vol. 2012, 2012.

[21] W. Fan, X. de Lisbona, F. Sun, J. Nielsen, M. Knudsen, and G. Pedersen, "Emulating spatial characteristics of mimo channels for ota testing," *Antennas and Propagation, IEEE Transactions on*, vol. 61, no. 8, pp. 4306–4314, 2013.

[22] D. Baum, J. Hansen, and J. Salo, "An interim channel model for beyond-3G systems: extending the 3GPP spatial channel model (SCM)," in *Vehicular Technology Conference, 2005. IEEE 61st*, vol. 5, 2005, pp. 3132–3136 Vol. 5.

[23] Y.-P. Zhang, P. Wang, Q. Li, and P. Zhang, "Hybrid Transform Coding for Channel State Information in MIMO-OFDM Systems," in *Communications (ICC), 2011 IEEE International Conference on*, 2011, pp. 1–6.

[24] Y.-P. Zhang, P. Wang, S. Feng, P. Zhang, and S. Tong, "On the efficient channel state information compression and feedback for downlink MIMO-OFDM systems," *accepted by IEEE Trans. Vehicular Technology*, 2013.

[25] "Verification of radiated multi-antenna reception performance of User Equipment," 3GPP, TR 37.977 V1.0.0, Sep. 2013.

[26] P. Kyosti and L. Hentila, "Criteria for physical dimensions of MIMO OTA multi-probe test setup," in *Antennas and Propagation (EUCAP), 2012 6th European Conference on*. IEEE, 2012, pp. 2055–2059.

Wei Fan received his Bachelor of Engineering degree in electrical engineering from Harbin Institute of technology, China, in 2009 and Master's double-degree with highest honors from Politecnico di Torino, Italy, and Grenoble Institute of Technology, France, in electronic engineering in 2011. From February 2011 to August 2011, he was with Intel Mobile Communications, Denmark. He is currently a Ph.D. candidate at Department of Electronic Systems at Aalborg University, Denmark. His main areas of research are over the air testing of MIMO terminals and radio channel modeling.

This article has been accepted for publication in a future issue of this journal, but has not been fully edited. Content may change prior to final publication. Citation information: DOI 10.1109/TAP.2014.2301179, IEEE Transactions on Antennas and Propagation

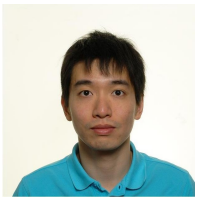

Fan Sun received the B.Eng. degree in telecommunication engineering with highest honors from Beijing University of Aeronautics and Astronautics (BUAA, now renamed as Beihang University), China, in 2007, the M.S. degree in wireless systems with highest honors from Royal Institute of Technology (KTH), Sweden, in 2009, the PhD degree from Aalborg University, Denmark, in 2013. From November 2008 to September 2009, he was with Ericsson Research, Sweden. From September 2009 to September 2010, he was with Nokia Siemens Network Research, Denmark. From June 2012 to December 2013, he was with Stanford University as a visiting student. He is currently a postdoc scholar in wireless communications at Stanford University. His research interests include multiple antenna techniques, cooperative communication, cross-layer design, and signal processing for communication systems.

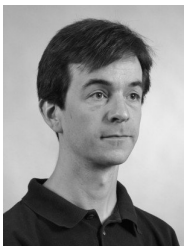

Jesper Ødum Nielsen received his master's degree in electronics engineering in 1994 and a PhD degree in 1997, both from Aalborg University, Denmark. He is currently employed at Department of Electronic Systems at Aalborg University where main areas of interests are experimental investigation of the mobile radio channel and the influence mobile device users have on the channel. He has been involved in MIMO channel sounding and modeling, as well as measurements using live GSM and LTE networks. In addition he has been working with radio performance evaluation, including over the air testing of active wireless devices.

Xavier Carreño received his Master degree from 'Escola Tènica Superior d'Enginyeria de Telecomunicació de Barcelona' (UPC) in 2011. At UPC he was deeply involved in baseband signal processing algorithms and MIMO OTA research topics within Intel Mobile Communications, where he currently has a leading role in the MIMO OTA development team as system engineer. He is involved in the standardization of MIMO OTA methods and has coauthored several 3GPP, CTIA and IC1004 contributions and several conference and journal papers on the subject. His primary interests are within the area of MIMO OTA testing techniques, MIMO channel modeling and LTE platform testing.

Jagjit Singh Ashta born in 1988, obtained a Master Degree in Telecommunications in the 'Escola Tènica Superior d'Enginyeria de Telecomunicació de Barcelona' (UPC) in 2012. In the same year he completed with honours his Master Thesis on MAC layer improvements for IEEE 802.11 networks (WLAN) at Aalborg University (AAU) in collaboration with Nokia Solutions and Networks (NSN). Currently he develops his career as a Wireless Communications Engineer at Xtel ApS and is employed as an external software consultant at Intel Mobile Communications, Denmark. His research interests cover the MAC and PHY layers of the RANs and the development of software solutions required to study them.

Mikael Bergholz Knudsen was born in 1964. He received the B.S. degree in electrical engineering from Aarhus Teknikum, Denmark, in 1989, and the M.S. and Ph.D. degrees from Aalborg University, Denmark, in 1992 and 2001, respectively. In 1993, he joined Maxon Telecom A/S, Aalborg, Denmark, where he designed RF circuitry for both analog and digital mobile phones. From 1998 to 2001, he worked as an industrial Ph.D. student for Siemens Mobile Phones A/S, Denmark, while he at the same time studied at Aalborg University. He is now with Intel Mobile Communications Denmark, where he is the project manager for the 4th Generation Mobile Communication and Test platform (4GMCT) and also the chairman of the steering committee for the Smart Antenna Front End (SAFE) projects; both sponsored by the Danish National Advanced Technology Foundation. His areas of interest include RF system design and handset antenna performance including more than one antenna. In the resent years one of his focus areas has been how to utilize the unique possibilities in the cooperation between university researchers and private companies. To support this effort he pursued and obtained an Executive-MBA in 2012 with focus on inter-organizational research strategies.

Gert Frølund Pedersen was born in 1965 and married to Henriette and have 7 children. He received the B.Sc. E. E. degree, with honour, in electrical engineering from College of Technology in Dublin, Ireland in 1991, and the M.Sc. E. E. degree and Ph. D. from Aalborg University in 1993 and 2003. He has been with Aalborg University since 1993 where he is a full Professor heading the Antenna, Propagation and Networking LAB with 36 researcher. Further he is also the head of the doctoral school on wireless communication with some 100 phd students enrolled. His research has focused on radio communication for mobile terminals especially small Antennas, Diversity systems, Propagation and Biological effects and he has published more than 175 peer reviewed papers and holds 28 patents. He has also worked as consultant for developments of more than 100 antennas for mobile terminals including the first internal antenna for mobile phones in 1994 with lowest SAR, first internal triple-band antenna in 1998 with low SAR and high TRP and TIS, and lately various multi antenna systems rated as the most efficient on the market. He has worked most of the time with joint university and industry projects and have received more than 12 M$ in direct research funding. Latest he is the project leader of the SAFE project with a total budget of 8 M$ investigating tunable front end including tunable antennas for the future multiband mobile phones. He has been one of the pioneers in establishing Over-The-Air (OTA) measurement systems. The measurement technique is now well established for mobile terminals with single antennas and he was chairing the various COST groups (swg2.2 of COST 259, 273, 2100 and now ICT1004) with liaison to 3GPP for over-the-air test of MIMO terminals. Presently he is deeply involved in MIMO OTA measurement.